1440 (1977); S. Weinberg, *ibid.* **40**, 223 (1978); F. Wilczek, *ibid.*, p. 279; J.-E. Kim, *ibid.* **43**, 103 (1979).
26. J. Preskill, M. Wise, F. Wilczek, *Phys. Lett. B* **120**, 127 (1983); L. Abbott and P. Sikivie, *ibid.*, p. 133; M. Dine and W. Fischler, *ibid.*, p. 137.
27. M. S. Turner, *Phys. Rep.* **197**, 67 (1990).
28. J. R. Primack, D. Seckel, B. Sadoulet, *Annu. Rev. Nucl. Part. Sci.* **38**, 751 (1988); P. F. Smith and J. D. Lewin, *Phys. Rep.* **187**, 203 (1990).
29. D. O. Caldwell, *Mod. Phys. Lett. A* **5**, 1543 (1990); K. van Bibber *et al.*, in *Trends in Astroparticle Physics*, D. Cline and R. D. Peccei, Eds. (World Scientific, Singapore, 1992), p. 154.
30. See, for example, F. Boehm and P. Vogel, *Annu. Rev. Nucl. Part. Sci.* **34**, 125 (1984).
31. P. J. E. Peebles, *Nature* **327**, 210 (1987); *Astrophys. J.* **315**, L73 (1987); R. Cen, J. P. Ostriker, P. J. E. Peebles, *ibid.* **415**, 423 (1993).
32. S. D. M. White, C. Frenk, M. Davis, *Astrophys. J.* **274**, L1 (1983); *ibid.* **287**, 1 (1983); J. Centrella and A. Melott, *Nature* **305**, 196 (1982).
33. See, for example, G. R. Blumenthal *et al.*, *Nature* **311**, 517 (1984); J. P. Ostriker, *Annu. Rev. Astron. Astrophys.* **31**, 689 (1993).
34. Q. Shafi and F. Stecker, *Phys. Rev. Lett.* **53**, 1292 (1984); A. van Dalen and R. K. Schaefer, *Astrophys. J.* **398**, 33 (1992); M. Davis, F. Summers, D. Schlegel, *Nature* **359**, 393 (1992); A. Klypin *et al.*, *Astrophys. J.*, in press.
35. A. Albrecht and A. Stebbins, *Phys. Rev. Lett.* **69**, 2615 (1992); D. Bennett *et al.*, *Astrophys. J.* **399**, L5 (1992); N. Turok, *Phys. Rev. Lett.* **63**, 2652 (1989); A. Gooding *et al.*, *Astrophys. J.* **372**, L5 (1991).
36. E. Aubourg *et al.*, *Nature* **365**, 623 (1993); C. Alcock *et al.*, *ibid.*, p. 621.
37. Supported in part by the Department of Energy (at Chicago) and by NASA (NAGW-2381) (at Fermilab).

RESEARCH ARTICLES

Multiple RNA Polymerase Conformations and GreA: Control of the Fidelity of Transcription

Dorothy A. Erie, Omid Hajiseyedjavadi, Mark C. Young, Peter H. von Hippel

Pre–steady state kinetics of misincorporation were used to investigate the addition of single nucleotides to nascent RNA by *Escherichia coli* RNA polymerase during transcription elongation. The results were fit with a branched kinetic mechanism that permits conformational switching, at each template position, between an activated and an unactivated enzyme complex, both of which can bind nucleotide triphosphates (NTPs) from solution. The complex exists most often in the long-lived activated state, and only becomes unactivated when transcription is slowed. This model permits multiple levels of nucleotide discrimination in transcription, since the complex can be "kinetically trapped" in the unactivated state in the absence of the correct NTP or if the 3′ terminal residue is incorrectly matched. The transcription cleavage factor GreA (or an activity enhanced by GreA) increased the fidelity of transcription by preferential cleavage of transcripts containing misincorporated residues in the unactivated state of the elongation complex. This cleavage mechanism by GreA may prevent the formation of "dead-end" transcription complexes in vivo.

Transcription of RNA is the first step in the chain of events leading to expression of the genetic information encoded in double-stranded DNA. The role of RNA polymerase in transcription is to synthesize, under the direction of the DNA template, the nascent RNA chain with high fidelity and at reasonable rates. The passage of the polymerase along the DNA template is uneven, with the "dwell time" at a given template position ranging from 10 ms to seconds or even minutes. These sequence-dependent differences in the transit rate of the polymerase along the template are "programmed" into the sequence in ways that are not yet understood. It is becoming apparent that these sequence-dependent dwell times comprise the central components of a regulatory network that controls gene expression at the level of transcription (*1*, *2*). Accordingly, it is important to identify all of the steps in the transcription pathway and to determine which might be rate limiting (and thus subject to regulation) for both correct and incorrect nucleotide incorporation.

The authors are at the Institute of Molecular Biology and Department of Chemistry, University of Oregon, Eugene, OR 97403.

Pre–steady state kinetic studies, which permit the characterization of the individual steps of an enzyme mechanism, should reveal the rate-limiting steps of the single nucleotide addition process of RNA synthesis, just as such studies have been used to elucidate DNA synthesis mechanisms. Kinetic studies of the single-nucleotide addition cycle of several DNA polymerases (*3*–*5*) have shown that the processive addition of a nucleotide residue to an elongating polynucleotide chain occurs stepwise (*2*) by (i) NTP binding, (ii) phosphotransfer, (iii) pyrophosphate product release, and (iv) translocation of the catalytic active site of the enzyme relative to the 3′ terminus of the growing chain. In addition, these studies have identified conformational changes that regulate the overall rate, fidelity, and processivity of nucleotide incorporation in DNA synthesis.

Application of quench-flow methods to studies of the pre–steady state kinetics (*6*) of RNA synthesis may not yet be practical, since some properties of stalled transcription elongation complexes differ even for complexes that have been purified by slightly different methods (*2*). Nevertheless, if selected steps of the single-nucleotide addition cycle are slowed, this process can be studied without a quench flow apparatus. Accordingly, we have used specific nucleotide misincorporation to probe the detailed mechanisms of nucleotide incorporation and discrimination in RNA synthesis catalyzed by *E. coli* RNA polymerase.

Misincorporation of a nucleotide residue increases the duration of certain steps of the nucleotide addition cycle from milliseconds to minutes. The slow rates of these processes permit the observation and study of conformational states of elongation complexes that may not be significantly populated during rapid synthesis, but which may be physiologically important in regulation, particularly for processes involving transcriptional pausing. We describe two experiments that provide sufficient information to define the mechanism of nucleotide discrimination at specific loci, as well as to identify several elementary steps in the overall nucleotide incorporation cycle. Experiments at other template positions suggest that our findings are likely to be general. The mechanism shares several features of the DNA polymerase single-nucleotide addition cycle, but the overall pathway differs in critical respects. Unlike the basically sequential (A → B → C) DNA polymerase mechanisms (*3*–*5*), our experiments indicate a branched kinetic pathway for RNA polymerase characterized by several alternative conformational states at each template position. The processivity and great stability of the transcription elongation complex allow us to observe kinetically the different conformational states that comprise the components of this branched pathway. These qualities ensure that the rates of change between conformational states are faster than the rate of

dissociation of the complex. The fact that equivalent states have not been observed in DNA synthesis may be due to the lower processivity of the examined DNA polymerases in that the dissociation of DNA polymerase–DNA complexes (*7*) may be faster than the rates of the equivalent conformational interconversions.

We have also examined the effects of the *E. coli* elongation accessory proteins NusA and GreA on misincorporation. NusA protein does not affect the observed misincorporation kinetics. In contrast, the mechanism we have deduced suggests, and experiments confirm, that the recently identified transcript cleavage factor GreA (*8*) enhances the fidelity of transcription. Furthermore, GreA appears to recognize nucleotide misincorporation in a manner similar to that of the (3′ → 5′) intrinsic exonuclease components of the DNA polymerases (*4*, *9*).

All experiments described in this article were performed with a DNA template that contains the λP_R promoter (*10*). The first 50 nucleotide residues of the transcript are

```
  +1
pppAUGUAGUAAGGAGGUUGUAUGGAA

+25          +35
 CAACGCAUAACCCUGAAAGAUUAC—
```

With this template, stable elongation complexes stalled at position +24 can be made by carrying out transcription in the absence of CTP (cytidine triphosphate); however, because of misincorporation at +25, some of the complexes read through to positions +25 and +27 (*11*). Consequently, we can measure the rate of misincorporation at +25, as well as the rate of extending past the misincorporated base to +27. We have performed a large number of experiments to examine the addition and removal (by pyrophosphorolysis and by protein factors) of correct and incorrect nucleotides at +25, +26, +27, and +28.

Three major transcripts 24, 25, and 27 nucleotides (nt) in length were observed during the time course of a transcription reaction initiated with 20 μM ATP, 20 μM UTP, and 3 μM [α-^{32}P]GTP (Fig. 1A) (*11*). The 27-nt transcript was sequenced and the dependence of misincorporation on nucleotide triphosphate (NTP) concentration was investigated. Uridine nucleotides were found to be misincorporated in place of cytosine nucleotides in all experiments. This finding is consistent with other in vitro and in vivo investigations of nucleotide misincorporation (*2*). In addition, the kinetics of nucleotide incorporation during the first 20 minutes of the reaction were independent (i) of ATP and GTP concentrations up to 1 mM (*12*); (ii) of pH between 6 and 9; (iii) of the presence or absence of pyrophosphate (100 μM), rifampicin or heparin, NusA, or sigma factors; and (iv) of the ratio of RNA polymerase to DNA template. However, the observed kinetics were dependent on the concentrations of UTP and GreA protein (see below).

We deduced the simplest kinetic scheme (Fig. 2) that can account for all the observed data (Fig. 1, A and B, and Fig. 3). A

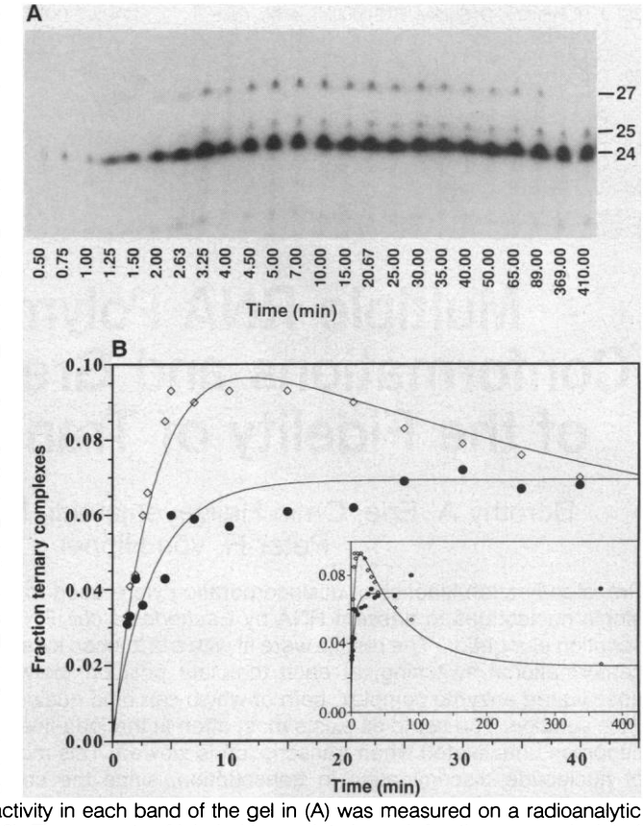

Fig. 1. (**A**) Distribution of the transcription products on a 20 percent acrylamide, 8 M urea gel as a function of time after the addition of 20 μM ATP, 20 μM UTP, and 3 μM [α-^{32}P]GTP (800 Ci/mmol). Reactions were done at 23°C in 30 mM Hepes buffer (pH 7.0), 200 mM potassium glutamate, acetylated bovine serum albumin (25 μg/ml), 10 mM magnesium glutamate, and 1 mM dithiothreitol, and were quenched with 80 percent formamide. The *E. coli* RNA polymerase holoenzyme (1 to 10 nM) and DNA (1 to 10 nM) were first incubated at 37°C for 10 minutes to allow open promoter complex formation and then at 23°C for 2 minutes before the addition of the NTPs. The lengths (in nucleotides) of the transcripts are shown on the left, and the times at which the reactions were stopped are shown below each lane. (**B**) Plots of the fraction of ternary complexes that have undergone a misincorporation event. The amount of radioactivity in each band of the gel in (A) was measured on a radioanalytic imaging system (AMBIS 4000). The amounts of labeled transcripts in each fraction were calculated by dividing the amount of radioactivity in the indicated band by the total amount of radioactivity in all bands corresponding to transcripts equal to or greater than 24 nt in length. Closed circles (●) indicate the terminally misincorporated 25-nt transcript; open diamonds (◇) indicate the internally misincorporated 27-nt transcripts. The curves were generated from the mechanism indicated in Fig. 2 with the computer program KINSIM (*35*). (Insert) The full time course of the reaction.

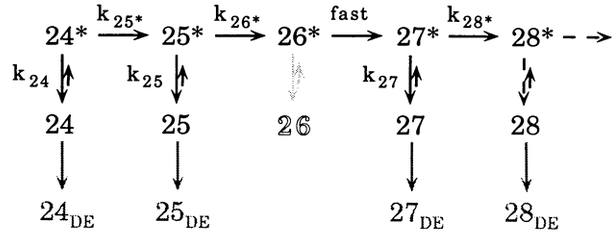

+1 +6 +25 +35
pppAUGUAGUAAGGAGGUUGUAUGGAACAACGCAUAACCC—
.....A 24 &24*
.....AU 25 &25*
.....AUAA 27 &27*
.....AUAAU 28 &28*

$k_{25*} = 5.5 \times 10^{-2}$ min^{-1} $k_{24} = 2.5 \times 10^{-1}$ min^{-1}
$k_{26*} = 8.0$ min^{-1} $k_{25} = 5.0$ min^{-1}
$k_{28*} = 1.2 \times 10^{-2}$ min^{-1} $k_{27} = 3.8 \times 10^{-3}$ min^{-1}
k_{25*} (20μM CTP) ≈ 6.0×10^{1} min^{-1}

Fig. 2. The kinetic mechanism deduced from the misincorporation experiment shown in Fig. 1. The numbers indicate the transcript position, and states n* and n represent an activated or an unactivated conformational state, respectively, of an elongation complex located at each position. The subscript "DE" indicates dead-end complexes. These transitions are shown in gray because they were not included in the mechanism used in the simulation. The transcript sequences as well as the pseudo-rate constants, k_n and k_{n*} (where n is the transcript length) (*36*), used to generate the kinetic curves in Fig. 1B are shown below the mechanism. In addition, an approximate pseudo-rate constant that would be expected for correct incorporation of CTP at +25 under these conditions is shown for comparison (*36*).

conformational model in which competitive productive and nonproductive NTP binding plays a central role is proposed (Fig. 4). We call this model the "kinetic trap" because the mechanism permits "trapping" of nucleotide misincorporation events. Evidence for each step in the mechanism is listed below.

1) The rates of production of the 25- and 27-nt transcripts exhibit multiphasic kinetics, and therefore the shapes of the curves cannot be reproduced on the basis of a simple sequential kinetic mechanism. Rather, the mechanism must include branch points or interconnecting parallel pathways. Experiments on the UTP dependence of misincorporation have shown that noninterconnecting parallel pathways also cannot simulate the kinetic data, and that multiphasic kinetics apply for all U for C misincorporation sites (Fig. 3).

2) Unlike misincorporation catalyzed by DNA polymerases, in which 100 percent misincorporation was observed for mutants lacking a 3′ → 5′ exonuclease activity, fewer than 20 percent of the complexes that reach +24 actually undergo a misincorporation event (Fig. 1B) (*4*). Since RNA polymerase does not dissociate from the elongation complex, this result can be explained only in terms of a conformational change that results in a species that does not misincorporate (24* → 24; Fig. 2), but that can be extended (chased) to full-length transcripts on the addition of all four NTPs (*13*).

3) After 10 minutes, the concentration of the 25-nt transcript remains constant, while that of the 27-nt transcript decreases because a second misincorporation permits extension to +28 (Fig. 1, A and insert in B). This result indicates that back reactions to +24 are not kinetically accessible under these conditions, and justifies equating their pseudo-rate constants to zero (Fig. 2).

4) The initial rate of appearance of the 27-nt transcript is equal to or slightly greater than that of the 25-nt species (Fig. 1B). Consequently, the rate-limiting step in the production of the internally misincorporated 27-nt transcript must be in the misincorporation step (24* → 25*) itself (at or before phosphodiester bond formation between the incorrect residue and the 3′ terminus of the nascent RNA), since both pyrophosphate release and translocation occur after misincorporation at +25 (Fig. 2). If some step after misincorporation at +25 were rate limiting, the rate of appearance of the 27-nt transcript would be slower than that of the 25-nt transcript.

5) Since the rate of appearance of the 27-nt transcript is as fast as that of the 25-nt species, it is necessary to invoke a conformational change (25* → 25) after misincorporation at +25 to account for the continued presence of any 25-nt product. Furthermore, the rate of this conformational change (25* → 25) must be similar to the rate of extension of the misincorporated transcript (25* → 26*) (Fig. 2).

6) We were able to determine not only the rate of misincorporation, but also the rate of chain extension from the misincorporated residue (Fig. 1, A and B, and Fig. 2). The simultaneous appearance of the terminally misincorporated 25-nt transcript and the internally misincorporated 27-nt transcript permits our determination of the rate of addition of the correct nucleotide residue (adenosine) at +26 onto the misincorporated residue at +25 (25* → 26*). The rate of extension of the misincorporated product is higher than the rate of the misincorporation step itself, but it is slower than extension from a correctly incorporated nucleotide residue (Fig. 2). Similar results have been observed for the DNA polymerase catalyzed extension of a mismatched nucleotide residue (*4, 5, 14*).

7) Since the slowest step in the reaction is incorporation of the incorrect base, and nucleotide removal is much too slow to be a factor under the conditions of this experiment, the conformational changes (24* → 24) and (25* → 25) must also be irreversible on the time scale of these experiments. If state 24* were in equilibrium with state 24, then all the complexes that reach +24 would eventually undergo misincorporation and continue to +27. An analogous conformational change at +27 (27* → 27) must also be included in the mechanism to fit subsequent kinetic observations (Figs. 1B and 2).

Nucleotide discrimination: Kinetic-trap and productive-nonproductive binding. We propose that the conformational change from state n* to state n (where n is the transcript length) represents a change from an activated (n*) to an unactivated (n) enzyme complex, and that the activated state results from "productive" binding of an NTP substrate, nucleotide incorporation, or both. By definition, the unactivated complex cannot catalyze the phosphotransfer reaction and, as demonstrated below, the activated complex can form a phosphodiester bond only if the NTP is bound to the enzyme with the correct geometry (productively) (Fig. 4).

This kinetic trap model (Fig. 4) combines properties of an induced-fit model (*15*) with those of a "productive-nonproductive binding" model to explain nucleotide selection during RNA synthesis by *E. coli* RNA polymerase. In an induced-fit model, the correct NTP substrate binds to the enzyme and induces a conformational change that allows rapid catalysis, while the incorrect NTPs bind, but induce the conformational change at a very slow rate, or not at all. In a productive-nonproductive binding model, nucleotide selection results from the different binding geometries of correct and incorrect NTP substrates (*16*). Specifically, the correct NTP binds with a configuration that results in catalysis (productive), and incorrect substrates bind with configurations that inhibit catalysis and also prevent a correct substrate from binding (nonproductive) (*16*). Both of these models have been invoked to explain nucleotide discrimination by DNA polymerases (*4, 9*). However, neither of these models alone can explain our kinetic data because (i) the productive-nonproductive binding model does not allow for

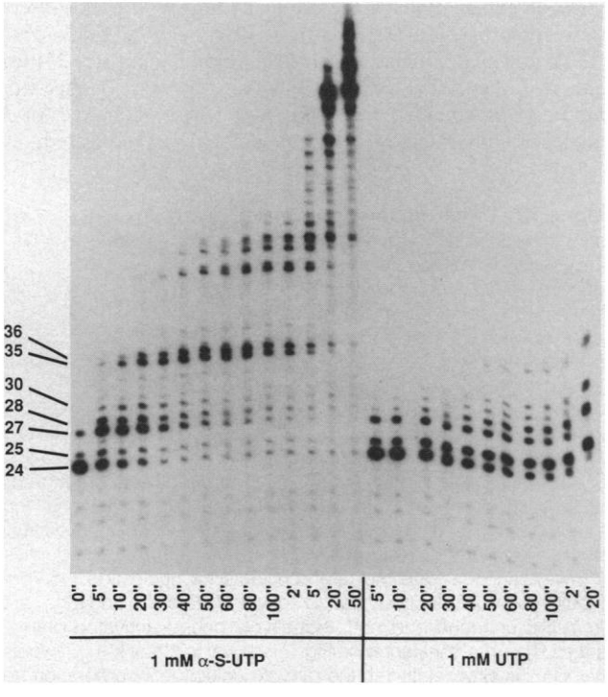

Fig. 3. A 20 percent acrylamide, 8 M urea gel of products from transcription reactions to which either 1 mM UTP (right) or 1 mM [α-S]UTP (left) was added; the time at which the reaction was quenched is included. The lengths of the transcripts are indicated on the left side of the gel. Zero time is at the time of the addition of UTP, which is 10 minutes after the start of the reaction. The reaction in the lane marked "0 seconds" was quenched 1 minute before the addition of either 1 mM UTP or 1 mM [α-S]UTP. The radioactivity was measured with AMBIS 4000.

conformational changes and (ii) the induced-fit model does not permit the NTPs bound to the activated state to be in direct equilibrium with NTPs in solution.

We extended the above concepts to generate a conformational model that allows for multiple levels of substrate selection. In this model, the unactivated state exhibits the same properties as in an induced-fit model, and the n → n* transition represents a conformational change like that described in induced-fit models (*15*). Specifically, such a change could bring the α-phosphorus of the NTP and the 3′-OH of the transcript into proper alignment for bond formation (*15*, *17*) or bring catalytic groups of the enzyme into correct relative positions (*15*). In contrast to the predictions of an induced-fit model, the activated state in our model is long-lived and can bind NTPs from solution both productively and nonproductively (*18*), but phosphodiester bond formation can occur in the activated state only if the NTP is bound productively. This model allows RNA polymerases with a correct, productively bound NTP to continue rapidly along the n* → (n+1)* pathway (Figs. 2 and 4), rather than entering the unactivated (n) states. Conversely, polymerases with an incorrect, nonproductively bound NTP cannot easily traverse this pathway, and consequently enter (are trapped) into unactivated states. Significantly, the n* → n transition serves as a kinetic trap for incorrect, but not for correct, substrates because it is irreversible only for the incorrect substrate. In this way, productive binding in the kinetic trap model (i) induces the n → n* conformational change, making the trap reversible for correct substrates; and (ii) permits bond formation in the activated state (n*), preventing the trap from "springing" on correct substrates. We discuss our data within this context below, and demonstrate that maintenance of fidelity in transcription elongation by RNA polymerase occurs at three different steps in the kinetic pathway: 24* → 24, 24* → 25*, and 25* → 25, and that conformational changes occur in all these steps.

The observed rate of decay 24* → 24 is similar to the rate of misincorporation 24* → 25* (Fig. 2), and neither of these rates is increased in the presence of 1 mM ATP or GTP (*12*). Accordingly, we propose that ATP and GTP both bind to the activated complex (24*) nonproductively, and that this nonproductive binding leads neither to phosphodiester bond formation (Fig. 4) nor to an enhanced rate of decay from state 24* to 24. In addition, the rate of reactivation of state 24 to 24* depends on both UTP and CTP concentrations, supporting the possibility that the conformational change from the unactivated (n) to the activated (n*) state is a result of productive binding (*19*). The conformational decay 24* → 24 (Fig. 2) represents the first of three levels of nucleotide discrimination within the single-nucleotide addition cycle in that complexes in state 24 can be considered to have prevented an error by trapping RNA polymerase before misincorporation.

Since complexes in state 24* are poised to undergo phosphotransfer, the mechanism of nucleotide discrimination in going from state 24* to 25* remains to be determined. As discussed above, the rate-limiting step for the incorporation of an incorrect base at +25 must be at or before phosphotransfer. To ascertain whether bond formation is rate limiting, we have substituted α-thio-UTP for UTP (Fig. 3). In general, if phosphotransfer were rate limiting, the rate of incorporation should be 60 to 100 times slower for the thio substrate than for the corresponding NTP (*20*). Replacement of thio- for oxo-phosphates in enzymatic phosphate transfer processes decreases the reaction rates 2 to 40 times (*21*). In contrast, the rate of nucleotide incorporation at +25 is significantly increased by replacement of UTP with α-thio-UTP (Fig. 3), making it highly unlikely that phosphodiester bond formation is the rate-limiting step for this misincorporation (*22*).

Accordingly, we propose that the incorrect nucleotide most often binds to the activated state nonproductively, and thus inhibits catalysis. Consequently, the (small) value of the ratio of productive to nonproductive binding constants (K_P*/K_{NP}*) governs the insertion of the incorrect NTP (Fig. 4). Such a geometric explanation has been proposed to account for a nucleotide discrimination ratio of about 10^4 for some DNA polymerases (*9*), and can also provide a simple explanation for the unusually high misincorporation rate of α-thio-UTP by RNA polymerase. The α-thio-UTP could enhance the rate of misincorporation by binding with a configuration that is preferable for phosphotransfer over that adopted by the oxo substrate (that is, K_P* for α-thio-UTP > K_P* for UTP) (Fig. 4). Alternatively, α-thio-UTP might bind less rigidly in the binding pocket than does the oxo analog, thereby potentially reducing K_{NP}* for α-thio-UTP and increasing the ratio K_P*/K_{NP}* for the thio substrate relative to that for UTP. The rate of misincorporation is enhanced by α-thio-UTP at all positions at which the template specifies CTP insertion (Fig. 3), suggesting that a productive-nonproductive binding model for nucleotide discrimination in n* states may be general for all uridine for cytosine misincorporation events. Such geometric effects in the activated state (n*) represent the second level of the nucleotide discrimination in the overall process that controls transcription fidelity.

Both the insertion of an incorrect nucleotide and the subsequent elongation of the nascent chain past the misincorporated residue are required to complete a misincorporation event. As mentioned above, the rate of extension from the incorrectly base-paired nucleotide is about ten times slower than that from a correctly paired nucleotide (Fig. 2). This decrease in rate is also consistent with the geometric discrimination model proposed above. In this case, however, it is the 3′ terminus of the transcript that is bound in the product terminus site with incorrect geometry for bond formation. Furthermore, the decay of state 25* → 25 is allowed by this reduction of the rate of chain extension (Fig. 2). This conformational decay is analogous to that proposed for state 24* → 24, except that the 25* → 25 transition represents the trapping of an error after its formation. These events of chain extension constitute the third stage of nucleotide discrimination during transcription.

Some of the complexes at +25 (as well as at +24) undergo a further conformational change from the unactivated state to an inactive (or dead-end) state that cannot be elongated, even in the presence of high

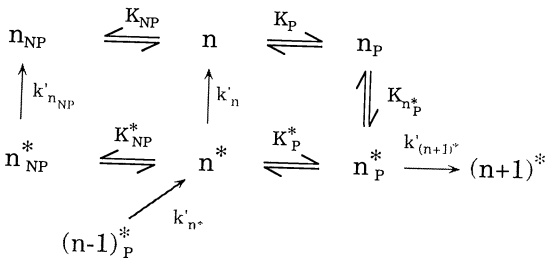

Fig. 4. The kinetic-trap model represented as equilibria between unbound and bound (productively and nonproductively) activated and unactivated states. The transcript length (or template position) is indicated by n. The synthesis pathway is represented by (n−1)* to n* to (n+1)*. Subscripts on n correspond to a bound NTP, where NP indicates a nonproductively bound NTP and P a productively bound NTP. K_P and K_{NP} are equilibrium constants for productive and nonproductive binding to the unactivated state, respectively. K^*_P and K^*_{NP} are equilibrium constants for productive and nonproductive binding to the activated state, respectively. Kn^*_P is the equilibrium constant for the equilibrium between the productively bound unactivated (n_P) and productively bound activated states (n^*_P). k′(n+1)* and k′n* are the rate constants for nucleotide incorporation (correct or incorrect) that results from a productively bound activated state. k′n and $k'n_{NP}$ are the rate constants for the decay from the unbound and nonproductively bound activated states to their respective unactivated states. The rate constant kn in Fig. 2 is equal to k′n + $k'n_{NP}$ if we assume that the rate of decay from n^*_P to n_P is slow relative to the rate of nucleotide incorporation from n^*_P to (n+1)*.

concentrations of all four NTPs, although both the RNA polymerase and the transcript remain bound to the DNA template (*23*, *24*) (Figs. 2 and 5). The probability of forming dead-end complexes is enhanced for complexes containing a terminally misincorporated residue (see chase reactions in Fig. 5). Unlike the dead-end complexes that form after the stalling of the polymerase by NTP depletion (*8*, *23*, *24*), the formation of the dead-end complexes observed in our study reflects the incorporation of an incorrect nucleotide residue at the 3′ end of the nascent RNA chain, rather than the lack of the next NTP, and represents "physiologically formed" dead-end complexes in *E. coli*. These dead-end complexes may correspond (i) to conformations that cannot undergo a conformational change to the activated state; (ii) to states in which the conformational change fails to bring the reacting groups into the proper positions for phosphotransfer; or (iii) to conformations in which the catalytic active center is displaced relative to the 3′ terminus, as has been suggested by Chamberlin (*25*).

Complexes that misincorporate, but do not elongate past the misincorporated residue (complexes in states 25 and 25_{DE}; Fig. 2), represent complexes that have made an error and have become trapped. The discovery of transcription cleavage factors GreA and GreB (*8*) provide a mechanism for reactivating such terminally misincorporated complexes.

Role of GreA in the fidelity of transcription. GreA and GreB are accessory proteins for *E. coli* RNA polymerase that promote the hydrolytic cleavage of the 3′ terminus of a nascent transcript when ternary complexes are stalled by nucleotide depletion (*26*). The resulting cleavage products are 2 to 10 nt long, and RNA polymerase appears to back up after the removal of these terminal nucleotides and reextend the shortened transcript (*8*, *27*, *28*). Both factors can prevent the formation of dead-end complexes by transcript cleavage (*29*), and GreB can reactivate dead-end complexes as well (*8*).

It has been suggested that the hydrolysis reactions promoted by GreA and GreB might be too slow, relative to the rate of elongation, to play a role in error correction (*28*). However, since the rate of extension of an incorrectly paired terminal nucleotide residue is significantly slower than that of a correctly paired residue, this slow rate of hydrolysis may be advantageous for the maintenance of low-cost fidelity in transcription by *E. coli* RNA polymerase. The slow hydrolysis catalyzed by GreA would make nucleotide excision of correctly paired nucleotides improbable, whereas significant excision of incorrect residues would be highly probable as a result of the longer dwell time of the complex at the site of a misincorporation. Similar proposals have been put forth to explain error recognition by the intrinsic exonuclease of DNA polymerases (*4*, *9*).

To test this hypothesis, we performed misincorporation experiments in the presence and absence of GreA (Fig. 5). In the presence of GreA, the appearance of terminally misincorporated products (25, 28, and 30 nt) is completely inhibited, but the rate of appearance of read-through products (27 and 29 nt) is only slightly reduced (Fig. 5). These data show that GreA does indeed increase the fidelity of transcription (>50 percent) by *E. coli* RNA polymerase and that GreA predominantly cleaves the transcript in the unactivated state of an elongation complex. If GreA primarily cleaved the transcript in the activated state, then there would be a concomitant reduction in the concentration of terminally and internally misincorporated products, since in the absence of GreA the rate of appearance of these products is approximately equal (see above and Figs. 2, 3, and 5). By contrast, if GreA cleaved only transcripts in the unactivated state and did so rapidly, the terminally misincorporated 25-, 28-, and 30-nt products might not be observed because they exist only in the unactivated or dead-end states, and the read-through 27- and 29-nt products would appear with approximately the same rate as in the control and then would be slowly cleaved as they decayed to their respective unactivated states. Accordingly, we propose that GreA preferentially recognizes and cleaves the unactivated state of an elongation complex. Our initial studies with GreB indicate that it also increases fidelity by an analogous mechanism. Furthermore, GreA may more rapidly cleave unactivated complexes that contain a mismatched 3′ end. Although attractive, this latter suggestion is not required to explain our observations since the rate of decay to the unactivated state is greater for complexes

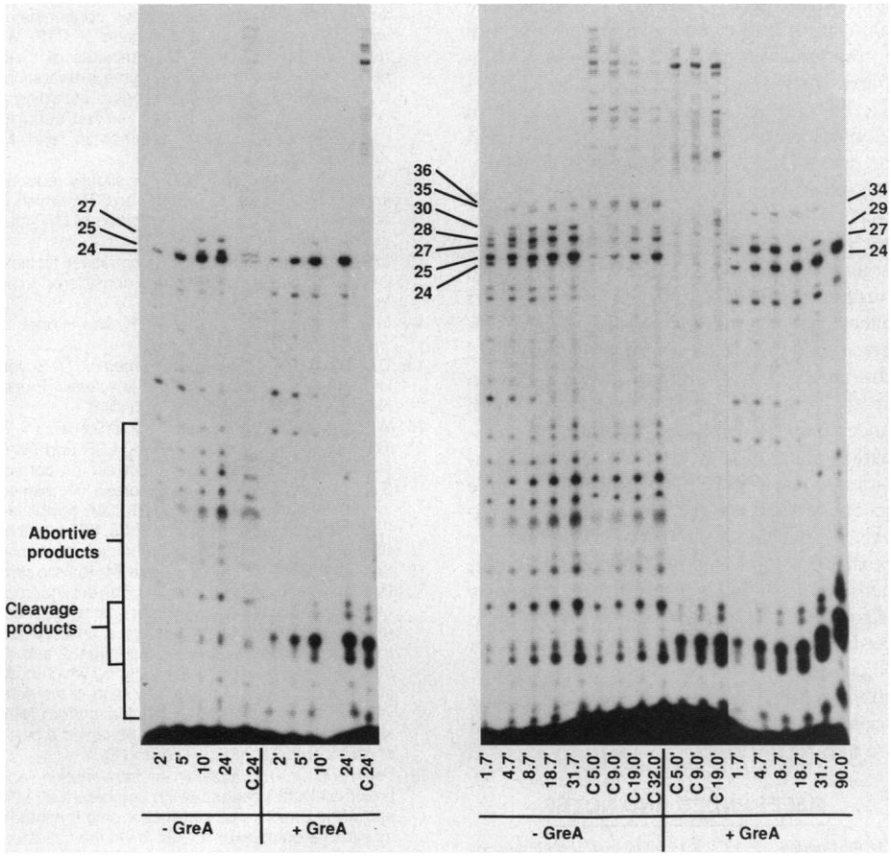

Fig. 5. Effect of GreA on misincorporation for both the unspiked (left panel) and the 1 mM UTP spiked (right panel) transcription reactions. Reactions were performed side by side in the presence and absence of GreA. At the designated times (bottom of gel) a portion of the reaction mixture was removed and either (i) quenched with formamide or (ii) extended by the addition of all four NTPs (chased) at 1 mM and were incubated for 30 minutes at room temperature. The time shown below each lane indicates the time of the quenching, or in the case of the chase reactions (denoted by a "C" preceding the time), the time at which the four NTPs were added. When included, GreA was in stoichiometric amounts and was added just before the NTPs were added. The sizes (see legend to Fig. 3) of the transcripts are marked on the left and right of the gel. The radioactivity in each band was measured with an AMBIS 4000.

with terminally misincorporated nucleotides than for those with correctly matched 3′ ends (Fig. 2). Since dead-end complexes are formed via the unactivated state (in our experiments), this proposal provides a simple explanation for the observation that GreA is able to prevent the formation of dead-end complexes (Fig. 5) (*8*) but is not able to rescue the same dead-end complexes once they have formed (*8*).

In addition to the rapid and preferential cleavage of terminally misincorporated products, GreA causes the internally misincorporated products (some of which have extended to +49) to slowly revert to +24 so that at 90 minutes all transcription complexes are at +24 and no additional misincorporation is observed (see 1 mM UTP spiked reactions in Fig. 5). If the function of GreA were simply to prevent the formation of dead-end complexes by cleavage, we would expect to reach a steady-state level of misincorporation or perhaps even to observe an increase in misincorporation because cleavage and subsequent reextension of the transcript would return the complexes to an activated state, thereby providing multiple chances for misincorporation at a single position. We conclude that GreA increases fidelity both by rapid cleavage of terminally misincorporated products and by slowly backing up (to +24) internally misincorporated complexes that have stalled one residue prior to a misincorporation site.

Since the overall extent of misincorporation is reduced in the presence of GreA, and since the terminally misincorporated 25-, 28-, and 30-nt transcripts are not observed (Fig. 5) (*30*), it is possible that GreA increases fidelity not only by cleavage of the misincorporated transcripts, but also by inhibiting the misincorporation process itself. This suggestion is consistent with the observation that when the time is long, all complexes are at +24 and no further misincorporation occurs (Fig. 5). In addition, the production of abortive transcripts in these experiments (Fig. 5), as well as with other promoters (*31*), is reduced in the presence of GreA. However, the rate of appearance of the 24 nt and longer transcripts are not significantly changed (Fig. 5), suggesting that it does not substantially increase either the rate of overall chain elongation or the rate of escape of RNA polymerase from the promoter. These results suggest that the function of GreA may be more complex than simply to cleave the transcript (*8*). It may produce more stringent nucleotide discrimination, confer additional stability onto the transcription complex (which is consistent with the reduction of abortive products), or both. It is possible that GreA enhances nucleotide discrimination, but it is clear that the presence of GreA greatly reduces the extent of nucleotide misincorporation by preferential recognition and cleavage of the unactivated state. The ability of GreB to reactivate and of GreA and GreB to prevent the formation of dead-end complexes may be important physiologically in error correction or in the reactivation of transcription complexes that have attained dead-end status due to misincorporation. These studies strongly suggest that an important function of these factors is to maintain transcriptional fidelity.

Multiple RNA polymerase conformations regulate transcription. We have presented experiments supporting a mechanism for misincorporation that is governed by the availability of alternative conformational states that can trap transcription complexes before and after a nucleotide has been misincorporated. We suggest that these conformational changes, which can manifest themselves at each template position, are the underpinnings of the mechanisms of transcriptional regulation during elongation as well as at termination. A significant amount of recent work on transcription elongation and pausing indicates that conformational properties of elongation complexes may play important regulatory roles (*2*, *24*, *32*). Conformational differences in elongation complexes can be large enough to be detectable by DNA and RNA footprinting experiments (*2*, *24*, *32*), and it may be that the mechanism we present here reflects such large-scale changes. Significantly, our ability to predict the effect of GreA on misincorporation, as well as to explain its effect on dead-end complex formation, suggests that we are beginning to understand the mechanism of transcription elongation at this detailed level of resolution. Such understanding will be essential for the elucidation of detailed mechanisms of gene regulation at the level of RNA transcription. We speculate that the transition to the unactivated state of the elongation complex may be the first step in many regulatory processes, perhaps including pausing, or that it may trigger the action of accessory proteins. Such conformational changes may also occur in eukaryotic RNA polymerases, since these enzymes may also exhibit more than one conformation at each template position and are also totally processive (*33*).

REFERENCES AND NOTES

1. R. Landick and C. Yanofsky, in *Escherichia coli and Salmonella typhimurium*, F. C. Neidhardt *et al.*, Eds. (American Society for Microbiology, Washington, DC, 1987), vol. 2, pp. 1276–1301.
2. D. A. Erie, T. D. Yager, P. H. von Hippel, *Annu. Rev. Biophys. Biomol. Struct.* **21**, 379 (1992).
3. S. S. Patel *et al.*, *Biochemistry* **30**, 511 (1991); M. J. Donlin *et al.*, *ibid.*, p. 538; M. E. Dahlberg and S. J. Benkovic, *ibid.*, p. 4835; B. T. Eger *et al.*, *ibid.*, p. 1441; T. L. Capson *et al.*, *ibid.* **31**, 10984 (1992).
4. I. Wong *et al.*, *ibid.* **30**, 526 (1991).
5. R. D. Kuchta *et al.*, *ibid.* **26**, 8410 (1987).
6. K. A. Johnson, *Methods Enzymol.* **134**, 677 (1986).
7. The kinetics of correct and incorrect incorporation by DNA polymerase from bacteriophage T4 have been investigated in the absence of its accessory proteins, which significantly increase the processivity and stability of the replication complex [N. G. Nossal, *FASEB J.* **6**, 871 (1992); M. C. Young, M. K. Reddy, P. H. von Hippel, *Biochemistry* **31**, 8675 (1992)]. Consequently, slow conformational changes in such holoenzyme replication complexes may not be accessible in studying the kinetics of the DNA polymerase alone.
8. S. Borukhov *et al.*, *Proc. Natl. Acad. Sci. U.S.A.* **89**, 8899 (1992); S. Borukhov *et al.*, *Cell* **72**, 459 (1993).
9. H. Echols and M. F. Goodman, *Annu. Rev. Biochem.* **60**, 477 (1991).
10. The template used in these studies was the linearized plasmid pDE 13. To generate this plasmid, we cloned the 3000-bp Bgl I fragment from pWT 2-8 (gift of M. Chamberlin, University of California, Berkeley), which contains the λP_R promoter with the λt_{R2} terminator approximately 500 bp downstream, with the Bgl I fragment of phagemid pBS$^-$ (Stratagene) which contains the f1 origin of replication. We then used Kunkel site-directed mutagenesis [T. A. Kunkel, *Proc. Natl. Acad. Sci. U.S.A.* **82**, 488 (1985)] to change the DNA base pair corresponding to position +6 of the λP_R transcript from a CG to a GC.
11. We have investigated misincorporation at a position requiring C rather than U because it is possible to obtain NTP stocks that are free from CTP; however, CTP stocks are always contaminated with UTP because of deamination of CTP. We have reproduced the first 30 minutes of these results with seven different enzyme preparations obtained from several laboratories, including a preparation reconstituted from purified subunits (gifts of R. Burgess, M. Chamberlin, and M. Kashlev and A. Goldfarb).
12. The rate of misincorporation was slightly reduced in the presence of 1 mM ATP or GTP, which is consistent with competitive inhibition of UTP misincorporation.
13. More than 80 percent of these complexes (in state 24) can be chased and thus are considered to be active.
14. M. K. Reddy, S. E. Weitzel, P. H. von Hippel, *J. Biol. Chem.* **267**, 14157 (1992).
15. D. E. Koshland Jr., in *The Enzymes*, P. D. Boyer, H. Lardy, K. Myrback, Eds. (Academic Press, New York, 1959), vol. 1, pp. 305–346.
16. W. P. Jencks, *Adv. Enzymol.* **43**, 219 (1975).
17. This suggestion is supported by ESR and NMR studies on the binding of incorrect or correct 3′-dNTPs to *E. coli* RNA polymerase complexed to single- and double-stranded DNA templates [G. L. Eichhorn *et al.*, *Biophys. J.* **59**, 565a (1991); G. L. Eichhorn, personal communication].
18. Since the rate of decay from state 24* to 24 is slow (minutes) relative to the rate of correct incorporation (0.05 to 1.0 s), the ternary complex must remain in the activated state for a finite period (dependent on k_n; see legends to Figs. 2 and 4) after nucleotide incorporation, during which both correct and incorrect NTPs may bind. If the activated state existed only when the correct NTP were bound, we would not have observed a burst of misincorporation (Fig. 1, A and B).
19. Ten minutes after initiation of transcription, approximately 100 percent of the complexes at +24 are in the unactivated state; after only 2 minutes most of the complexes at +24 are in the activated state. Consequently, if we add 1 mM UTP to the reaction at 2 or 10 minutes, we can measure the rate of misincorporation from the activated or unactivated state, respectively. We have found that the kinetics of misincorporation do not depend on whether 1 mM UTP is added to the reaction at 2 minutes or at 10 minutes after the addition of 20 μM ATP, 20 μM GTP, and 3 μM [α-^{32}P]GTP. This result indicates that UTP can induce the transition 24 → 24*, and that at 1 mM UTP, misincorporation (24* → 25*) is slower than reactivation (24 → 24*). In addition, high concentrations of UTP are required to reactivate the

complexes, whereas very low concentrations of CTP (10 nM) are sufficient for reactivation.
20. S. J. Benkovic and K. J. Schray, in *The Enzymes*, P. D. Boyer, Ed. (Academic Press, New York, ed. 3, 1971), vol. 8, pp. 201–238.
21. D. Herschlag, J. A. Piccirelli, T. R. Cech, *Biochemistry* **30**, 4844 (1991).
22. It is possible, but unlikely, that the enzyme stabilizes the thio transition state relative to the oxo transition state, which would result in a rate enhancement when the oxo derivative is replaced with the thio derivative. Consequently, phosphate transfer could be rate limiting; however, no such effect has been observed with other enzymes (*20, 21*).
23. J. R. Levin and M. J. Chamberlin, *J. Mol. Biol.* **196**, 61 (1987).
24. B. Krummel and M. J. Chamberlin, *ibid.* **225**, 221 (1992); *ibid.*, p. 239.
25. M. J. Chamberlin, *The Harvey Lectures* (Series 88, Wiley-Liss, New York, in press).
26. Whether GreA itself cleaves the transcript or whether GreA enhances an activity that is intrinsic to RNA polymerase is not clear (*8, 27*).
27. C. K. Suratt, S. C. Milan, M. J. Chamberlin, *Proc. Natl. Acad. Sci. U.S.A.* **88**, 7983 (1991).
28. G. A. Kassevetis and E. P. Geiduschek, *Science* **259**, 944 (1993).
29. The eukaryotic transcription factor SII exhibits similar "backing up" activity; however, this backing-up process, at least in some cases, involves the sequential removal of mononucleotides from the 3′ end of the transcript [D. Wang and D. K. Hawley, *Proc. Natl. Acad. Sci., U.S.A.* **90**, 843 (1993)]. These authors suggested that SII may play a role in preserving fidelity during transcription. This view represents an alternative to the suggestion that the function of GreA, GreB, and SII (or an activity stimulated by SII, GreA, or GreB) is to *rescue* dead-end complexes (*8, 34*). This role appears to be the only one that has been explored for GreA and GreB, even though dead-end complexes do not appear to be normally formed by *E. coli* RNA polymerase in transcription reactions in which all four NTPs are present throughout the initiation and elongation phases (*8, 23, 24*). In contrast, dead-end complexes of RNA polymerase II, which can be rescued by SII, have been observed in the presence of all four NTPs at attenuation sites in vitro (*34*).
30. We have not observed the formation of the 25-nt product in the presence of GreA even as early as 15 seconds after the addition of 1 mM UTP.
31. R. Landick and G. Feng, personal communication.
32. C. L. Chan and R. Landick, in *Transcription Mechanisms and Regulation*, J. Conaway and R. Conaway, Eds. (Raven Press, New York, in press).
33. H. Matsuzaki, G. A. Kassavetis, E. P. Geiduschek, *J. Mol. Biol.*, in press.
34. D. Reines, *J. Biol. Chem.* **267**, 2795 (1992); M. G. Izban and D. S. Luse, *Genes Dev.* **6**, 1342 (1992).
35. B. A. Barshop, R. F. Wrenn, C. Frieden, *Anal. Biochem.* **130**, 134 (1983).
36. We use the term pseudo-rate constant because (i) the reactions are pseudo–first order and (ii) the NTP concentrations are below those that yield V_{max}. The constants were determined for the concentrations used in this experiment (Fig. 2). The constant for correct incorporation was estimated for the temperature and the NTP concentrations used, based on our measurements and those of G. Rhodes and M. J. Chamberlin [*J. Biol. Chem.* **249**, 6675 (1974)].
37. We dedicate this paper to the memory of Harrison (Hatch) Echols, whose clear thinking about, and elegant descriptions of, fidelity mechanisms in DNA replication significantly inspired our studies and interpretations. Supported, in part, by USPHS research grants GM-15792 and GM-29158 (P.H.vH.), by USPHS postdoctoral fellowships GM-12915 (D.A.E.) and AI-07568 (M.C.Y.), by a grant from the Lucille P. Markey Charitable Trust, and by an American Cancer Society Research Professorship of Chemistry (P.H.vH.). We thank C. Chan, R. Landick, and G. Eichhorn for sharing unpublished manuscripts; E. Baldwin, C. Chan, M. Chamberlin, G. Eichhorn, and R. Landick, as well as several laboratory colleagues, for helpful discussions; and C. Chan, G. Feng, and R. Landick for providing us with purified GreA and GreB proteins.

11 May 1993; accepted 21 September 1993

Guanidinium Chloride Induction of Partial Unfolding in Amide Proton Exchange in RNase A

Stephen L. Mayo† and Robert L. Baldwin‡

Amide (NH) proton exchange rates were measured in 0.0 to 0.7 M guanidinium chloride (GdmCl) for 23 slowly exchanging peptide NH protons of ribonuclease A (RNase A) at pH* 5.5 (uncorrected pH measured in D_2O), 34°C. The purpose was to find out whether GdmCl induces exchange through binding to exchange intermediates that are partly or wholly unfolded. It was predicted that, when the logarithm of the exchange rate is plotted as a function of the molarity of GdmCl, the slope should be a measure of the amount of buried surface area exposed to GdmCl in the exchange intermediate. The results indicate that these concentrations of GdmCl do induce exchange by means of a partial unfolding mechanism for all 23 protons; this implies that exchange reactions can be used to study the unfolding and stability of local regions. Of the 23 protons, nine also show a second mechanism of exchange at lower concentrations of GdmCl, a mechanism that is nearly independent of GdmCl concentration and is termed "limited structural fluctuation."

Whether hydrogen-deuterium (H-D) exchange in proteins occurs by partial unfolding has been debated hotly (*1*). Classic experiments (*2*) indicate that the NH proton exchange rates of bovine pancreatic trypsin inhibitor (BPTI) depend on a global thermodynamic property of the protein. The exchange rates of individual NH protons were compared for a family of proteins homologous to BPTI, either from different species or from chemically modified variants produced, for example, by reducing and blocking a specific disulfide bond. The exchange rates of all measured NH protons could be correlated closely with T_m, the midpoint of the thermal transition for global unfolding, suggesting that exchange rates depend on global thermodynamic behavior. In contrast, experiments over many years have suggested that some exchange reactions may occur by partial unfolding (*1*). Still other experiments and lines of reasoning (*3*) have suggested (*1*) that exchange reactions may occur by limited structural fluctuations involving solvent penetration, analogous to the mechanism by which oxygen penetrates myoglobin to reach its binding site on the heme iron.

To obtain new evidence on this question, we used two-dimensional proton nuclear magnetic resonance (2D ^{1}H-NMR) to measure exchange rates of individual NH protons in RNase A as a function of the concentration of guanidinium chloride (GdmCl). Guanidinium chloride causes protein unfolding by interacting with the unfolded protein, and the change in Gibbs energy upon unfolding varies linearly with the molarity (M) of GdmCl. The slope, $-m$, of the plot of Gibbs energy as a function of the molarity of GdmCl is proportional to the number of GdmCl interaction sites exposed on unfolding (*4*), which is taken to be proportional to the surface area exposed. We make use of this fact to ask whether H-D exchange of individual peptide NH protons can be caused to occur by partial unfolding by means of adding GdmCl. For our conditions, exchange is known to occur by the EX2 exchange mechanism (*1, 5*) that is defined below. This means that the apparent change in Gibbs energy, ΔG_i^*, for the conformational reaction that permits exchange can be obtained for each proton by the relation

$$\Delta G_i^* = -RT\ln\left(\frac{k_{HX}(i)}{k_c(i)}\right) \quad (1)$$

where $k_{HX}(i)$ is the observed rate constant for exchange of proton i and $k_c(i)$ is the chemical exchange rate when proton i is fully solvent exposed, obtained from model peptide data (*6*). The conversion of H-D exchange rates to Gibbs energies is possible because in the EX2 exchange mechanism

The authors are in the Department of Biochemistry, Stanford University School of Medicine, Stanford, CA 94305.

†Present address: Division of Biology, California Institute of Technology, Pasadena, CA 91125.
‡To whom correspondence should be addressed.